Korean J. Chem. Eng., 36(11), 1869-1881 (2019)
DOI: 10.1007/s11814-019-0389-5

pISSN: 0256-1115
eISSN: 1975-7220

Rapid synthesis of phytogenic silver nanoparticles using *Clerodendrum splendens*: its antibacterial and antioxidant activities

Aarcha Jayakumar† and Radha Kuravappulam Vedhaiyan

Bioproducts Lab, Department of Chemical Engineering, A.C. Tech., Anna University, Chennai 600 025, India
(*Received 18 May 2019 • accepted 16 September 2019*)

Abstract−Silver nanoparticles (AgNPs) were rapidly green synthesized using *Clerodendrum splendens* (*C. splendens*) leaf extract with an environment-friendly approach. The stability, morphology and grain size of the AgNPs were determined using Zeta potential analysis, Transmission electron microscopy (TEM) and X-ray diffraction spectra (XRD). The phytochemicals present in the *C. splendens*, which are responsible for the bioreduction of silver ions (Ag^+ ions) and stabilization of AgNPs, were investigated using Fourier transform infrared spectroscopy (FTIR). The vital compositions in the AgNPs solution were analyzed by energy dispersive X-ray spectroscope (EDS). Using X-ray photoelectron spectroscope (XPS) measurement, the effect of *C. splendens* extract on the formation of AgNPs was investigated. The surface area of the AgNP was evaluated by using multiple point Brunauer-Emmett-Teller (BET) method. Results indicated that a low concentration of leaf extract is enough to enhance the rate of formation of AgNPs. *C. splendens* instantaneously reduced Ag^+ to AgNPs to reach 98% yield within 15 min. The fabricated AgNPs are in the size range of ~46 nm, well crystallized with face-centered cubic (fcc) symmetry. The AgNPs revealed a significant antimicrobial activity against airborne pathogens such as *Pseudomonas aeruginosa* (*P. aeruginosa*) and *Bacillus subtilis* (*B. subtilis*).

Keywords: Silver Nanoparticles, *Clerodendrum splendens*, Leaf Extract, Antibacterial, Antioxidant

INTRODUCTION

Nanoparticles, due to their unique properties, have gained more prominence in technology areas such as the medical sector [1], chemical sector [2], and environmental protection [3]. Generally, there are two main approaches for nanoparticle synthesis: top-down approach and bottom-up approach. The top-down approach includes numerous methods such as mechanical milling, laser ablation, nanolithography, sputtering, and thermal decomposition. The common bottom-up methods for the nanoparticles synthesis are sol-gel, chemical vapor deposition, pyrolysis, and biosynthesis [4].

In the recent years, the biosynthesis of nanoparticles has received great attention [5]. Biosynthesis is a green method and a potential alternative to other nanoparticle synthesis methods, as it is cost-effective, simple, environmentally friendly, non-toxic, and can easily be produced in the required amount. Biosynthesis uses biological agents such as bacteria, fungi, and plant extracts to synthesize nanoparticles. Amongst them, plant-based nanoparticle synthesis can be simple and beneficial over other biological agents as it reduces the complicated process of maintaining fungi or bacterial cell cultures.

Plant leaves are cheap and easily available. In addition, most of the plant leaves are withered and being wasted in our day to day life. In this study, we effectively made use of the withered leaves of *C. splendens* to synthesize AgNPs for the first time. AgNPs is a good metal of choice, as they possess antibacterial, antiviral, and antifungal activity [6]. The AgNPs possess oligodynamic effect and act on the target sites extracellularly and intracellularly [7].

Most research studies on the fabrication of AgNPs have been done using plant leaves. Some well known examples include synthesis of AgNPs using aqueous leaf extract of *Nigella arvensis* (Love in a mist) [8], *Eucalyptus globulus* (Eucalyptus) [9], *Swertia chirayita* (Chirata) [10], *Leucas aspera* (Tamba) [11], *Clome Gynandra* (Shona cabbage) [12]. However, these studies employ hot water extraction method for the preparation of plant leaf extract. Such leaf extraction method involves boiling the fresh leaves in water for about 15-30 min, which often modifies the characteristics of the underlying phytochemicals. In this study, we followed a different approach, namely, the plant tissue homogenization method (PTH), for the extraction of the phytochemicals because the efficiency of plant extract to reduce metal ions is highly dependent on the type of phytochemical extraction method. This method involves grinding of leaves, soaking in water for about two hours, and finally straining the water-soaked leaves [13]. We remark that the leaf extract prepared via PTH is obtained in raw state and it is better than the hot water extraction method as it prevents the phytochemical modification caused due to the boiling action.

Our present work studied the fabrication of AgNPs using *C. splendens* leaf extract. Additionally, enhancement of their antioxidant and antibacterial activity against airborne microbes are reported in this study. We selected *C. splendens* for its cost-efficiency and easy availability.

C. splendens is an evergreen climber or running shrub belonging to the family verbenaceae [14]. Its common name is Flaming Glorybower [15]. It is native to Western Africa and is widely distributed in the tropical regions throughout the world. The leaves contain reducing sugars, glycosides, unsaturated sterols, triterpenoids,

†To whom correspondence should be addressed.
E-mail: aarchajay@gmail.com

and flavonoids [16]. The plant is used in traditional medicine to treat wounds and burns [17], haemorrhoids, diarrhea and dysentery [18]. Previous studies have reported that the *C. splendens* leaf extract has antioxidant, antimicrobial and anti-inflammatory properties [19].

MATERIALS AND METHODS

1. Materials

Silver nitrate ($AgNO_3$) was purchased from Central Drug House (CDH), India, and was of analytical grade. *C. splendens* leaves were collected from the surroundings of Chennai, Tamil Nadu, India. Double distilled water was used throughout the study.

2. Preparation of PTH and HW Leaf Extract

2-1. PTH Method

The collected *C. splendens* leaves were thoroughly washed and dried. The clean leaves were ground to fine particles. 10 g of these fine particles was soaked in 100 mL of distilled water for 2 h and centrifuged at 5,000 rpm for 15 min to obtain a clear supernatant of the plant extract. The resulting solution was filtered through Whatman filter paper grade No. 1 (Pore size: 11 μm) for filtering the fine particles present in the extract. The obtained leaf extract was stored at ambient temperature (30 °C) for further use.

2-2. HW Method

Here, the clean leaves were cut into fine particles. 10 g of these finely cut clean leaves was boiled in 100 mL of distilled water at 60 °C for 20 min, and then the extract was filtered through Whatman filter paper grade No. 1 (Pore size: 11 μm). The obtained leaf extract was stored at ambient temperature (30 °C) for further use.

3. Synthesis of Silver Nanoparticles

To estimate the reduction of Ag^+ ions, 10 mL of freshly prepared leaf extract was added to 100 mL of 1 mM $AgNO_3$. The reaction was carried out in a dark room to decrease the photoactivation of $AgNO_3$ at an ambient temperature of 30 °C. Within a short period, the color of the resulting solution started changing from light green to colloidal brown indicating the formation of AgNPs. The solution containing AgNPs was centrifuged at 15,000 rpm for 15 min to obtain a pellet of AgNPs. The pellet was washed with distilled water to get rid of biomass residue and then dried in the oven at 60 °C for 24 h, which was used for further studies. The experimental conditions reported in this paper were obtained by optimizing the capacity of *C. splendens* leaf extract to reduce Ag^+ ions to AgNPs. The qualitative evaluation of the aqueous leaf extract as a reducing agent was as per the method reported by Ahmed et al. [20]. The reaction kinetic of AgNPs synthesized via *C. splendens* extract at different time intervals was studied.

4. Characterization of Silver Nanoparticles

Bioreduction of Ag^+ ions was monitored using UV visible (UV-vis) spectrophotometer (Perkin Elmer Lambda 25) at different time intervals. The spectrum of AgNPs colloidal solution at different time intervals was recorded on spectrophotometer in the range 200-800 nm. Zeta potential analysis of AgNPs was on Melvern Nano ZS (Malvern Instrument Ltd., UK). Size and morphology of the synthesized AgNPs were observed using a transmission electron microscope (TEM Model: Philips CM200). Sample for the TEM analysis was prepared by drop-coating the AgNPs solutions onto carbon coated copper TEM grids. XRD measurement was used to confirm the crystalline pattern of the synthesized AgNPs. XRD pattern was recorded by drop casting the colloidal silver solution onto a glass slide with Rigaku DMAX 2200 diffractometer using monochromatic Cu Kα radiation running at 40 kV and 30 mA. EDS analysis was used to analyze the elemental composition of the AgNPs. The phytochemical constituents present in the plant extract responsible for the stabilization and capping of the bio-reduced AgNPs were characterized by FTIR analysis. FTIR spectra of the leaf extract and AgNPs were measured after drying 50 μl of the solution on a cesium iodide plate at room temperature. XPS measurement was done on ESCALAB 250 X-ray photoelectron spectrometer to examine the effect of *C. splendens* extract on the formation of AgNPs. The surface area of the AgNPs at liquid nitrogen temperature (77.4 K) was estimated with BET surface area analyzer (Model 2200e, Quantachrome Instruments) by using multiple point BET method.

5. Antibacterial Activity

Well diffusion assays were used to assess the antibacterial potential of the synthesized AgNPs. *P. aeruginosa* (ATCC 27853) and *B. subtilis* (ATCC 21332) were the test strains. Overnight grown bacterial culture was swabbed on the solidified nutrient agar plate. After swabbing, wells were punched at the required places of the plate. The samples were prepared by mixing 1 mg of AgNPs in 1 mL of distilled water, which was further diluted to final concentrations of 5, 10, and 15 μg/mL in distilled water. 50 μL from each sample was then loaded into the wells followed by incubation at 37 °C overnight. The leaf extract was used as the blank and Amoxicillin 500 mg was used as the control.

6. Determination of Growth Curve

A study on the growth of bacteria (*P. aeruginosa* and *B. subtilis*) exposed to AgNPs and the leaf extract was done. Five mL of bacterial culture was added to 200 mL of nutrient broth. The culture was incubated at 37 °C and shaken at 150 rpm for 24 h. The samples were prepared by dispersing 1 mg of AgNPs in 1 mL of distilled water separately, which were diluted to final concentrations of 15 μg/mL bacterial cultured broth. The leaf extract was used as a control and distilled water as a blank. Growth rates were determined by measuring optical density (OD) at 600 nm through time series.

7. Antioxidant Activity

A slightly modified method of Brand-Williams et al. [21] was used to study the free radical-scavenging activity of AgNPs and leaf extract using DPPH. Ascorbic acid was used as a standard reference material. In this procedure, 1 mg of AgNPs, leaf extract, and ascorbic acid were mixed in 1 mL of distilled water separately, which were diluted to final concentrations of 5, 10, 15 μg/mL. One mL of each diluted sample was added to 4 mL of 0.1 mM DPPH ethanol solution. The mixtures were shaken and kept at room temperature for 30 min. The DPPH in ethanol solution was used as the control and ethanol as the blank. The absorbance of the solutions was determined at 517 nm using a UV-Vis spectrophotometer. The antioxidant activity (AA%) percentage was calculated using the formula

$$AA(\%) = \frac{A_{control} - A_{sample}}{A_{control}} \times 100, \quad (1)$$

where $A_{control}$ is the absorbance of 0.1 mM DPPH ethanol solution,

A_{sample} is the absorbance of the samples. All experiments were done in triplets and their mean values are presented along with ±standard deviation.

RESULTS AND DISCUSSION

1. Mechanism of AgNPs Formation

The synthesis of AgNPs, mediated by plants, relies mainly on the presence of the phytochemicals. *C. splendens* extract contains reducing sugars, glycosides, unsaturated sterols, triterpenoids, and flavonoids [16], which are the typical phytochemicals responsible for the reduction of Ag^+ ions. Among them, the flavonoids are the strongest reducing agents that can directly scavenge the reactive oxygen species [22], and they immediately facilitate the reduction of Ag^+ ions to AgNPs. The mechanism involved in the biosynthesis of AgNPs is shown in Fig. 1. The flavonol reduces Ag^+ ions and it gets converted to the enolform (see Fig. 1(a)) resulting in the formation of AgNPs. Proteins present in the plant leaf extract apparently reduce Ag^+ ions to AgNPs and then stabilize the resulting nanoparticles by forming a protein coating on it (Fig. 1(b)).

2. Synthesis of AgNPs

The AgNPs were synthesized using PTH leaf extract of *C. splendens*. The Ag^+ ions were observed to show a rapid reduction by 9.09%w/v *C. splendens* leaf extract in the $AgNO_3$ solution (i.e., concentration ratio of leaf extract: $AgNO_3$ is 0.1 : 1), which confirms that the PTH *C. splendens* leaf extract is an active reducing agent for AgNPs synthesis. Due to the reduction phenomenon, within 1 min, the color of the PTH colloidal solution changed from light green to reddish brown, which indicates the initiation of the AgNPs formation (see Fig. 2(a)). The brown color is due to the excitation of the surface plasmon vibrations in the AgNPs [23]. This result is found to be promising compared to previous studies [8-10]. For the HW method, using the same leaf extract (9.09%w/v *C. splendens*), such a rapid reduction was not observed, wherein, the colloidal solution color changed from pale yellow to reddish brown (Fig. 2(d)) after 5 min. Therefore, these results indicate that the initiation of the AgNPs synthesis by PTH leaf extract is observed faster compared to HW leaf extract, and this may be due to the presence of greater amounts of unmodified phytochemicals in the PTH leaf extract than in the HW leaf extract.

2-1. Reaction Kinetics

The reaction kinetics of AgNPs synthesized using PTH and HW leaf extracts was studied at fixed concentrations of $AgNO_3$ and *C. splendens* extract, under varying time intervals. The $AgNO_3$ solution was taken as the control. The intensity of the peaks at 420 nm of control and AgNPs at varied time intervals observed using UV-vis spectroscope is shown in Table 1. The yield of AgNPs synthesized via *C. splendens* was calculated using Eq. (2). The Residual Ag^+ concentration in the reaction solution was expressed as in Eq. (3).

$$\text{Yield}\,(\%) = \frac{\text{420 nm peak intensity of AgNPs solution}}{\text{420 nm peak intensity of control}} \times 100 \quad (2)$$

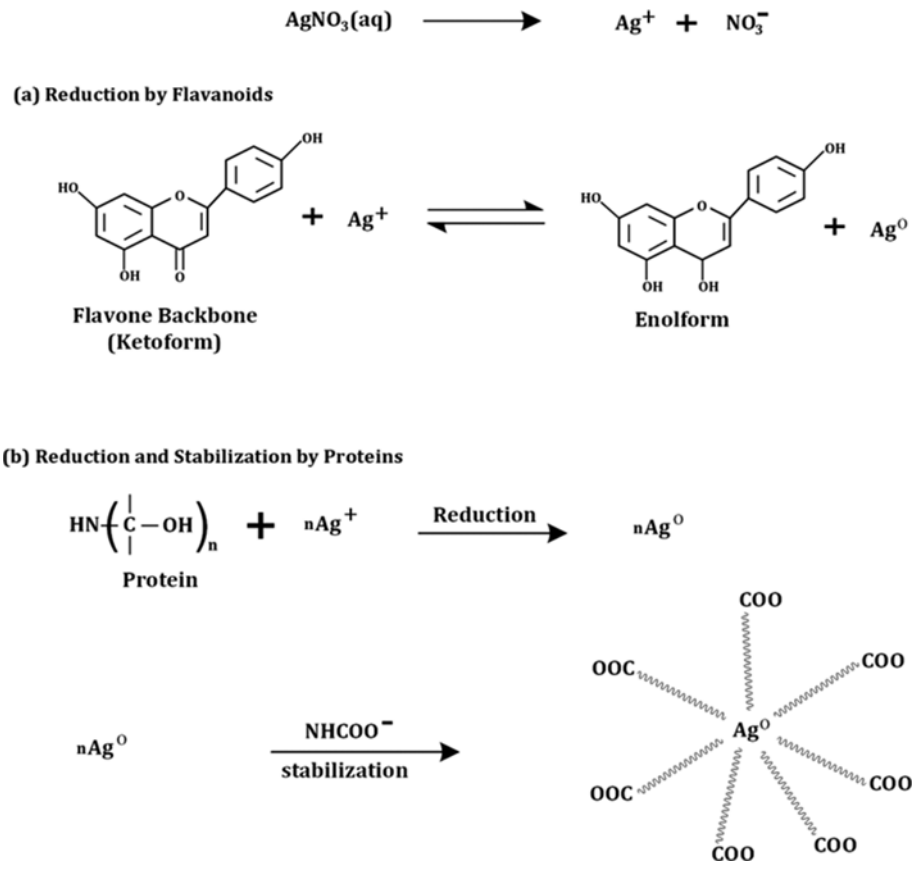

Fig. 1. The mechanism involved in the biosynthesis of AgNPs.

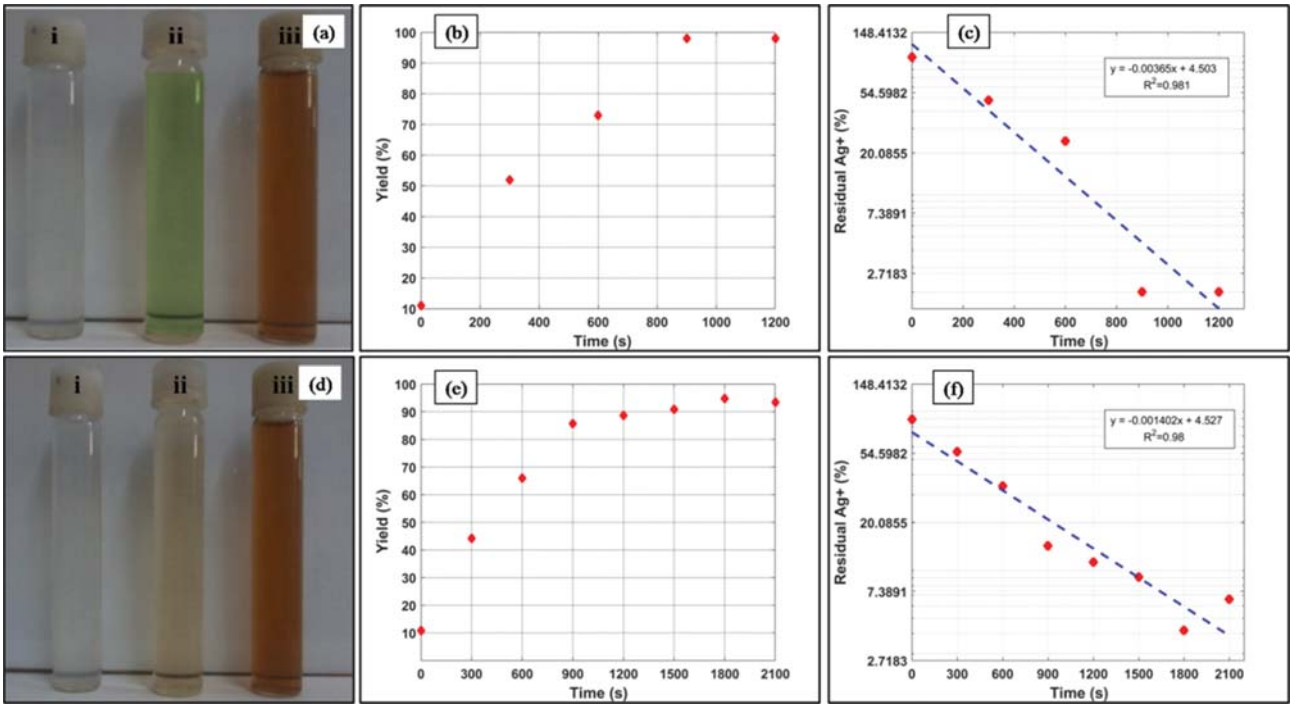

Fig. 2. PTH method: (a) Visual photograph of (i) 1 mM $AgNO_3$ (ii) *C. splendens* leaf extract (iii) AgNPs solution (b) Yield of AgNPs with time (c) Residual Ag^+ concentration with time. HW method: (d) Visual photograph of (i) 1 mM $AgNO_3$ (ii) *C. splendens* leaf extract (iii) AgNPs solution (e) Yield of AgNPs with time (f) Residual Ag^+ concentration with time.

Table 1. The intensity of peak at 420 nm of AgNPs at different time intervals

S. No.	Sample	AgNPs at time (sec)	Peak intensity at 420 nm
1	AgNPs using PTH *C. splendens*	0	0.11
		300	0.519
		600	0.629
		900	0.98
		1200	0.98
2	AgNPs using HW *C. splendens*	0	0.108
		300	0.442
		600	0.68
		900	0.857
		1200	0.887
		1500	0.909
		1800	0.958
		2100	0.934
3	$AgNO_3$	Control	1.00

$$\text{Residual } Ag^+ (\%) = 100 - \text{Yield} \quad (3)$$

The yield of AgNPs via PTH *C. splendens* increased exponentially with reaction time up to 15 min and after which it attained a steady-state (Fig. 2(b)). The AgNPs yield% obtained using PTH *C. splendens* was 98%. The yield of AgNPs using HW *C. splendens* increased up to the reaction time of 30 min and then slightly decreased (Fig. 2(e)). The yield% of AgNPs using HW *C. splendens* was 94%. The natural logarithm of Ag^+ concentration decreased linearly with the reaction time, according to Fig. 2(c) and 2(f), with large excess in the leaf extract concentration suggesting a pseudo-first-order kinetic for the reduction reaction. However, the concentration of Ag^+ ions at the initial of the reaction time (0 min) determined by the intercept of the fitted line x=0 was 90.01%. Hence, the concentration of Ag^+ ions was not 100% at the reaction beginning, indicating that Ag^+ ions were reduced into AgNPs instantaneously. The reaction rate constant determined by the slope of fitted line was 3.65×10^{-4} s^{-1} and 1.4×10^{-4} s^{-1} for PTH and HW leaf extract, respectively. This indicates that the AgNPs synthesis rate using PTH *C. splendens* is faster compared to HW *C. splendens*. Therefore, we conclude that the nature of *C. splendens* extract plays a major role in the reduction of Ag^+ ions into AgNPs over time.

3. UV-visible Spectral Analysis

The UV-vis spectra of the colloidal AgNPs solution is given in Fig. 3, which shows a strong and broad surface plasmon resonance (SPR) band at 420 nm for different time intervals. In Fig. 3(a) the absorbance peak intensity of 0.98 a.u. at 420 nm of AgNPs prepared with PTH extract remained steady after a reaction time of 15 min, indicating the completion of the reaction. Therefore, in our experiment, the analysis was stopped after 20 min. The rapid completion of synthesis reaction in 15 min was found to be advantageous compared to those previous studies [8-10] that reported several hours for the completion of AgNPs synthesis. The absorbance of AgNPs synthesized with HW extract (Fig. 3(b)) increased up to the reaction time of 30 min after which it is slightly decreased to 0.934 a.u. A similar result was noticed in the previous report [8] that used HW leaf extract of *Nigella arvensis* to synthesize AgNPs.

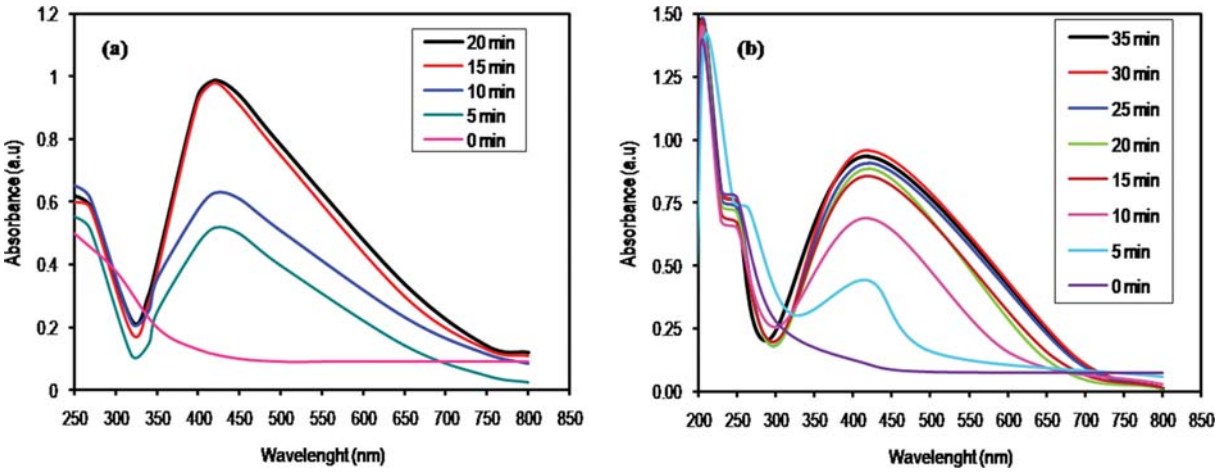

Fig. 3. UV-Visible spectra of AgNPs synthesis via (a) PTH leaf extract (b) HW leaf extract.

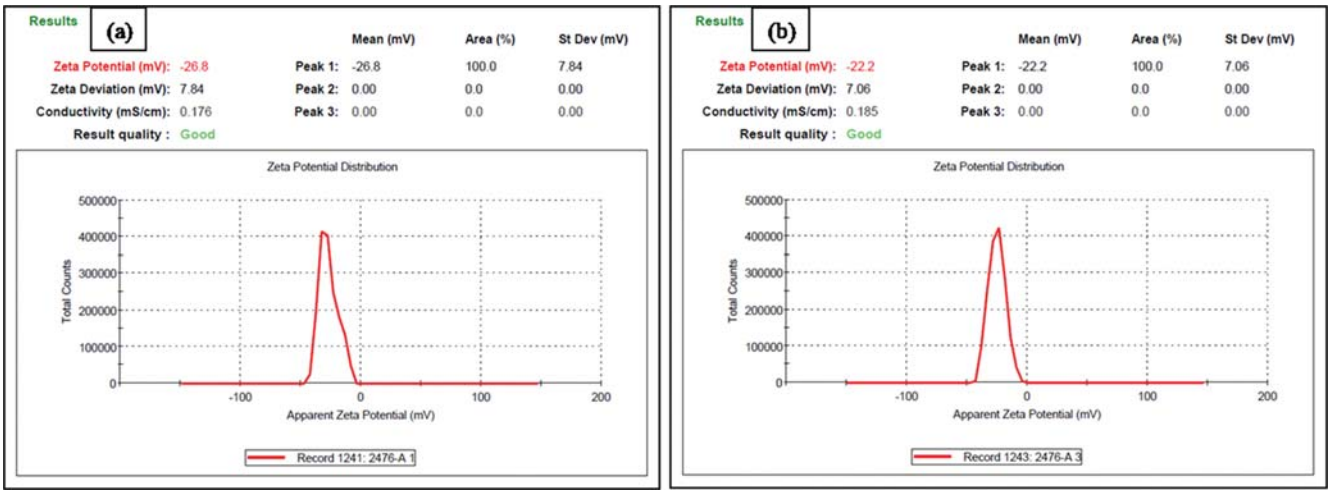

Fig. 4. Zeta potential of AgNPs prepared with (a) PTH leaf extract (b) HW leaf extract.

From the above comparative study using UV-vis spectra, the absorbance peaks of AgNPs synthesized with PTH leaf extract are more intense and stable with time than those synthesized using HW leaf extract. This is possibly due to a larger amount of reducing and stabilizing biomolecules present in the PTH extract compared to the HW extract.

The presence of the SPR band is due to the combined vibrations of electrons of AgNPs in resonance with lightwave [24]. The concentration of the AgNPs in the colloidal solution can be computed through Beer-Lambert's law, according to which absorbance (A) is directly proportional to the product of the concentration of the absorbing species (C) and the path length (L), which can be defined by the equation as $A=\log10(1/T)=\varepsilon CL$, where ε is the molar absorptivity [25]. Therefore, increase in the intensity of the absorbance peak indicates an increase in the concentration of the AgNPs in the colloidal solution [26]. At the time of reaction completion, the absorbance of PTH AgNPs is higher compared to that of HW AgNPs revealing a better yield of PTH AgNPs. The steady position of absorption peak in the UV-vis spectrum confirms that new particles do not aggregate. The broad peak is a characteristic of larger silver nanoparticles. Therefore, the optical properties reveal that the completion of the AgNPs synthesis using PTH extract is faster with a better yield of AgNPs than that of HW extract. The results obtained from UV-vis spectrum are in good agreement with the TEM micrographs.

4. Zeta Analysis

We investigated the stability of AgNPs synthesized using PTH and HW leaf extract. Fig. 4 shows the zeta potential value of AgNPs in the colloidal solution. In general, nanoparticles with zeta potential value lesser than −25 mV are stable [27]. From Fig. 4(a), the zeta potential value of the PTH AgNPs is −26.8 mV and, hence, they are stable and not prone to rapid aggregation. On the other hand, the AgNPs synthesized with HW leaf extract (Fig. 4(b)) exhibit a zeta potential value greater than −25 mV, thereby indicating the incipient stable nature of the nanoparticles that are prone to aggregation. Therefore, nanoparticles prepared with PTH extract were more highly stable than that of HW extract, revealing more stabilizing constituents in PTH leaf extract. These results are promising compared to those reported previously [10,28] that showed less stable nanoparticles with zeta potential value greater than −25 mV.

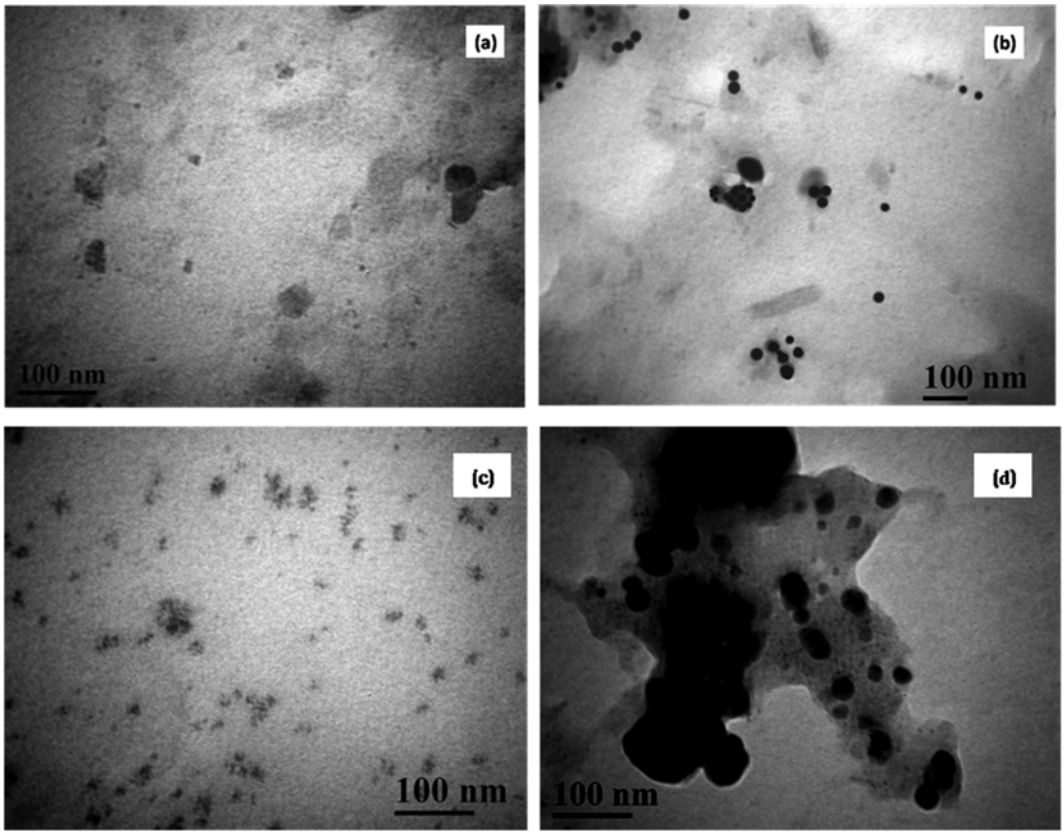

Fig. 5. TEM images of AgNPs prepared with PTH leaf extract at reaction time (a) 5 min (b) 15 min and HW leaf extract at (c) 5 min (d) 35 min.

We remark that the negative surface charge of AgNPs was attributed to deprotonation of the protein's carboxylate group (-COO-) in the *C. splendens* leaf extract surrounding the AgNPs surface [29]. The negatively charged surface of AgNPs effectively stabilized the nanoparticles via electrostatic repulsive force.

5. TEM Analysis

TEM analysis confirmed the formation of AgNPs. Fig. 5 shows the TEM micrographs of AgNPs at different reaction times. It is evident from Fig. 5(b) that the PTH AgNPs are spherical with little aggregation. The AgNPs prepared by *C. splendens* extract had an average size of 46±5 nm. The nanoparticles are monodisperse, which is an important property when considered for commercial applications. However, the HW leaf extract was reported to react with Ag^+ ions to produce mostly aggregated nanoparticles of various shapes (spherical and cubical) with an average particle size of ~58 nm. Their wider size range of 15-100 nm indicates polydisperse property. The TEM results revealed that the PTH leaf extract produces smaller AgNPs of uniform shape and size than that of HW leaf extract. Previous studies on AgNPs synthesis reported producing wider size range of 10-100 nm particles by *Cladosporium cladosporioides* [30], 85-120 nm AgNPs by *Swertia chirayita* [10] and bigger size AgNPs of ~92 nm by *Bacillus persicus* [28]. From Fig. 5((a), (c) and (b), (d)), the size of the AgNPs increases with the reaction time. Fig. 5(b) and (d) show a thin organic layer surrounding the AgNPs, suggesting that the constituents present in the leaf extract act as a capping organic agent.

6. Comparison with Various Studies on Silver Nanoparticles Synthesis Using Biomolecules

Table 2 shows the AgNPs synthesis using various biomolecules with regard to the production time and the characteristics of AgNPs. The biomolecules extracted from various biosources, such as bacteria, fungi, algae, and plants, are widely used in the production of AgNPs. In contrast to plants, bacteria and fungi are contagious, which is an important disadvantage when it comes to safety. *Bacillus* strains such as *Bacillus pumilis* and *Bacillus lichenformis* are acutely toxic for humans [31]. *Cladosporium cladosporioides* are pathogenic and can cause chronic allergy and asthma [32].

C. splendens is an evergreen plant that it is widespread throughout the world [14]. Therefore, *C. splendens* leaves are easily available from the surroundings and cost-effective. In our study, *C. splendens* leaves were stored at room temperature for a whole day without its deterioration. Refrigeration of *C. splendens* leaves at 4 °C maintained freshness for a week. All bacterial and fungal strains have to be stored in a sterile environment to prevent contamination. *Penicillium* sp. [33] has been studied extensively as it led to the discovery of antibiotics, but it is very expensive [34] compared to *C. splendens*. *Padina boergesenii* is a marine alga [35] that is not easily available and is expensive compared to *C. splendens*. Storage of *Padina boergesenii* is complicated, as it has to be kept in an ice-box [35] to prevent deterioration. *Nigella arvensis* is a deciduous plant and thus its leaves are not easily available throughout the year. *Eucalyptus globulus* is an evergreen plant, but it is not suitable for

Table 2. Comparison of various studies on the biosynthesis of AgNPs regarding production time and characteristics of AgNPs

PREVIOUS REPORTS					
Biosource	Sample	Biomolecules extraction (Methods)	Time for AgNPs synthesis and concentration (UV-Visible)	AgNPs shape and size (TEM/SEM)	Stability (Zeta Analysis)
Bacteria	*Bacillus pumilus* [28]	• Isolation and cultivation time of strain is overnight • Biomolecules extraction time is 24 h	• AgNPs synthesis time is 72 h • The absorbance is nearly 2 a.u.	• AgNPs were spherical, cubical, triangular and hexagonal in shape • Size: ~80 nm • Particles are mostly aggregated	• Zeta potential value: −18.5 mV
	Bacillus persicus [28]	• Isolation and cultivation time of strain is overnight • Biomolecules extraction time is 24 h	• AgNPs synthesis time is 48 h • The absorbance is greater than 1 a.u.	• AgNPs were spherical and hexagonal in shape • Size: ~92 nm • Particles were moderately aggregated	• Zeta potential value: −16.6 mV
	Bacillus licheniformis [28]	• Isolation and cultivation time of strain is overnight • Biomolecules extraction time is 24 h	• AgNPs synthesis time is 48 h • The absorbance is nearly 2 a.u.	• AgNPs were spherical, triangular, and hexagonal in shape • Size: ~77 • Particles are mostly aggregated	• Zeta potential value: −21.3 mV
Fungi	*Cladosporium cladosporioides* [30]	• Time for the production of biomass and biomolecules extraction is 1 week	• AgNPs synthesis time is 48 h • The absorbance is nearly 2 a.u.	• AgNPs were spherical, and cubical in shape • Size: 10-100 nm (Polydisperse) • Particles are aggregated	----
	Penicillium sp. [33]	• Production time of biomass is 8 days • Biomolecules extraction time is 72 h	• AgNPs synthesis time is 72 h • The absorbance is less than 0.8 a.u.	• AgNPs were spherical, triangle, and pyramidal in shape • Particles are aggregated	• Zeta sizer: Average size is 130.5 nm
Algae	*Padina boeregesenii* [35]	• HW extraction • Biomolecules extraction time is 20 min	• AgNPs synthesis time is 120 min • The absorbance is higher than 1.5 a.u.	• AgNPs were spherical in shape • Size: ~43.3 nm • Particles are aggregated	----
Plants	*Nigella arvensis* [8]	• HW extraction of dried leaves • Biomolecules extraction time is 30 min	• AgNPs synthesis time is 120 min • The absorbance is less 0.8 a.u.	• AgNPs are spherical and cubical in shape • Size: 5-100 nm (Polydisperse) • Particles are aggregated	---
	Eucalyptus globulus [9]	• HW extraction at 80 °C • Biomolecules extraction time is 30 min	• AgNPs synthesis time is 10,080 min • The absorbance higher than 1 a.u.	• AgNPs are spherical, triangular and hexagonal in shape • Size: 30-50 nm • Particles are aggregated	---
	Swertia chirayita [10]	• Soxhlet extraction • Biomolecules extraction time is 6-8 h	• AgNPs synthesis time is 240 min • The absorbance less than 0.4 a.u.	• AgNPs are spherical, cubical and irregular in shape • Size: 85-120 nm (Polydisperse) • Particles are aggregated	• Zeta potential value: −15 mV

Table 2. Continued

PRESENT REPORT					
Biosource	Sample	Biomolecules extraction (Methods)	Time for AgNPs synthesis and concentration (UV-Visible)	AgNPs shape and size (TEM/SEM)	Stability (Zeta Analysis)
Plant	*Clerodendrum splendens*	• PTH extraction • Biomolecules extraction time is 2 h 15 min	• AgNPs synthesis time is 15 min • The absorbance is 0.98 a.u.	• AgNPs are spherical in shape • Size: 46±5 nm (Monodisperse) • Particle are little aggregated	• Zeta potential value: −26.8 mV
		• HW extraction • Biomolecules extraction time is 20 min	• AgNPs synthesis time 35 min • The absorbance is 0.934 a.u.	• AgNPs are spherical and cubical in shape • Size: 15-100 nm (Polydisperse) • Particle are aggregated	• Zeta potential value: −22.2 mV

cultivation at altitude below 1,200 m or at altitude where snowfall is heavy [36], which is an important drawback when considering its availability.

The biomolecules from algae and plants are extracted by various methods such as plant tissue homogenization, hot water, and Soxhlet extraction. PTH method, used for the extraction of biomolecules from *C. splendens*, is energy-saving and it is possible to acquire most of the constituents present in plant parts including the thermo-labile constituents [13] which are the key factors for the rapid production of AgNPs. HW biomolecule extraction method, used for *C. splendens*, *Nigella arvensis* [8], *Eucalyptus globulus* [9], and *Padina boergesenii* [35], is rapid but the extraction of thermo-labile constituents is not feasible. Soxhlet method, used for *Swertia chirayita* leaf [10], is time and energy-consuming when compared to HW and PTH method. The biomolecule extraction from bacteria and fungi is time-consuming and complicated as it typically involves various steps such as isolation and culturing of strains [28,30,35].

The synthesis of AgNPs using the PTH *C. splendens* is very fast (15 min) compared to that of other methods of biomolecules from plant, algae, bacteria and fungi. TEM analysis revealed that PTH *C. splendens* produced AgNPs of uniform shape and size. Zeta potential analysis revealed that PTH *C. splendens* produced AgNPs with better stability compared to other methods of biomolecules. Most bacteria, fungi, and algae produce a high concentration of AgNPs, but the particles are mostly aggregated, which is an important drawback when it comes to stability. They produce much larger nanoparticles. Among the bacterial species, *Bacillus persicus* produces less stable AgNPs in colloidal solution. The comparison study in Table 2 reveals that the PTH leaf extract of *C. splendens* shows better results in regard to human safety, availability, AgNPs synthesis, stability, and characteristics. Therefore, AgNPs synthesized using PTH *C. splendens* is preferred for further studies.

7. XRD Analysis

The XRD pattern of AgNPs is shown in Fig. 6. The figure shows characteristic peaks of silver at 2θ values of 38.82°, 44.93°, 64.96°, and 77.72°, which may be, respectively, assigned to the diffraction from (111), (200), (220), and (311) lattice planes of the face-centered cubic (fcc) structure of silver [37]. This XRD pattern is in correspondence with the standard XRD pattern of metallic silver JCPDS no. 04-0783 [38].

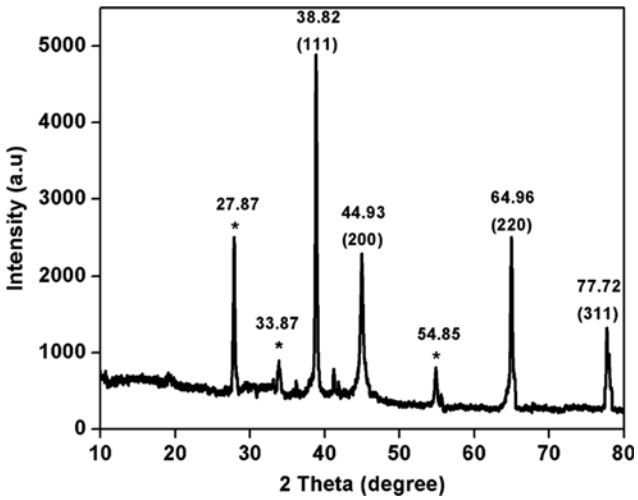

Fig. 6. XRD pattern of AgNPs.

The average grain size of synthesized AgNPs is determined using the Debye-Scherrer equation [39] as follows:

$$d=(K\lambda/\beta\cos\theta\ \pi), \quad (4)$$

where d is the size of AgNPs (nm), K is a shape factor (0.9 assumes spherical crystallites), λ is the wavelength of the X-rays (0.154184 nm for copper radiation), β is the FWHM of diffraction angle (in radians), and θ is the half of the Bragg angle (in radians).

The average grain size of AgNPs from XRD spectrum is calculated to be 46 nm in Table 3. The XRD analysis confirms the crystalline nature of the AgNPs. However, some unidentified peaks, denoted using (*), are seen in Fig. 6, which may be due to the

Table 3. Average grain size of AgNPs from XRD spectra

Sample	2θ (Degree)	(hkl)	Grain size, D (nm)	Average size, D (nm)
AgNPs	38.82	111	42.15	~46
synthesized using	44.93	200	43.02	
C. splendens	64.96	220	47.13	
	77.72	311	51.05	

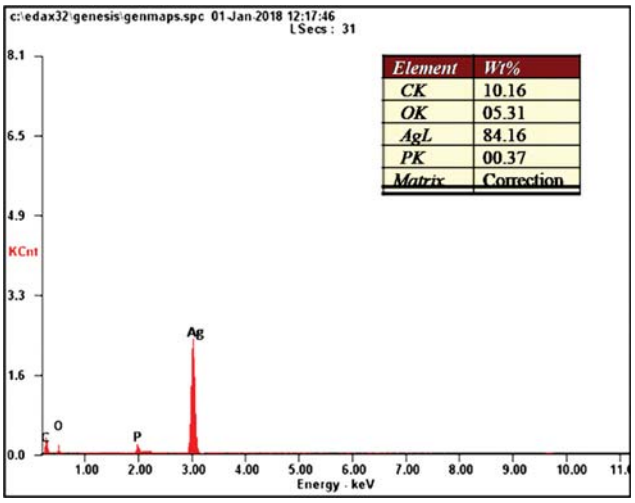

Fig. 7. EDS spectrum of AgNPs.

organic compounds present in the leaf extract.

8. EDS Analysis

EDS analysis was performed to examine the elemental composition of the green synthesized AgNPs. The EDS spectrum is shown in Fig. 7, in which the intense peak at 3 keV is typical of the metallic AgNPs [40]. The spectrum also shows the presence of carbon, phosphorous and oxygen, which may be due to various phytochemicals present in the leaf extract. The compositions obtained from EDS analysis were silver 84.16%, carbon 10.16%, oxygen 5.31% and phosphorous 0.37%. This quantitative analysis revealed the presence of high silver content in the sample.

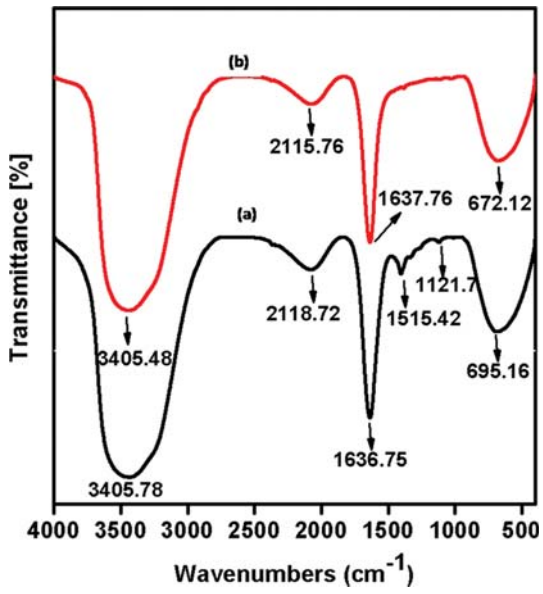

Fig. 8. FTIR spectra of (a) *C. splendens* leaf extract (b) AgNPs.

9. FTIR Analysis

FTIR spectroscopy analysis characterized the functional groups present in the leaf extract, which were efficient for the reduction of Ag^+ ions to AgNPs and capping of the phyto-reduced AgNPs. The FTIR spectrum is shown in Fig. 8. The figure shows the comparison on FTIR spectra of (a) leaf extract and (b) AgNPs. The broad peaks at 3,405.78 cm^{-1} and 3,405.48 cm^{-1} are the characteristic of O-H stretching of hydroxyl groups [41,42]. The bands observed at 2,118.72 cm^{-1} and 2,115.76 cm^{-1} correspond to -C≡C stretching of alkynes groups [41]. The strong bands at 1,636.75 cm^{-1} and 1,637.76 cm^{-1} correspond to C=C vibration of aromatic structures, C=O stretching of amide I and carboxylic acids [43,44]. The peak at 1,515.42 cm^{-1} corresponds to C-C stretching (in ring) of the aromatic group and at 1,121.7 cm^{-1} was attributed to the -C-O stretching vibrations of polyols [45]. The bands at 695.16 cm^{-1} and 672.12 cm^{-1} might be attributed to primary and secondary amines and amides. The disappearance of peaks at 1,515.42 cm^{-1} and 1,121.7

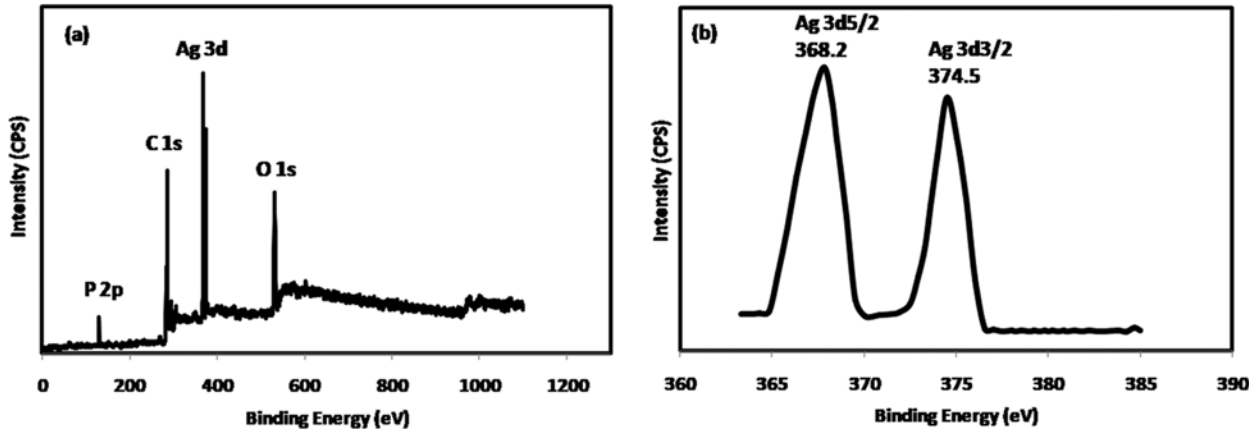

Fig. 9. XPS spectra of AgNPs (a) Survey spectrum (b) Ag3d core level spectrum.

cm^{-1} for AgNPs indicates that the polyols such as flavonoids, terpenoids, and polysaccharides are primarily responsible for the reduction of Ag^+ ions. This observation agrees with the results obtained by Hadi et al. [46]. The shift of peak from 695.16 cm^{-1} to 672.12 cm^{-1} indicates that the amine components are involved in the reduction of Ag^+ ions to AgNPs and in the stabilization of the resulting AgNPs [47,48]. Thus, we conclude that flavonoids and terpenoids present in the *C. splendens* are highly responsible for the formation and stabilization of AgNPs.

10. XPS Analysis

Fig. 9 shows the XPS spectra of AgNPs produced using *C. splendens* extract. The XPS survey spectrum (Fig. 9(a)) confirms the presence of P2p, O1s, C1s, and Ag3d core levels. The Ag3d core level spectrum (Fig. 9(b)) shows narrow peaks of Ag3d5/2 and Ag3d3/2 occurring at the binding energies 368.2 and 374.5 eV, respectively [49]. From this, we arrive at the following conclusions: i) the Ag^+ are reduced to metallic AgNPs; ii) the presence of other elements (P2p, O1s, C1s) may be due to various phytochemicals present in the *C. splendens* leaf extract. We remark that the presence of elements obtained from the XPS analysis agrees well with the result given by the EDS analysis.

11. BET Analysis

The BET plot of AgNPs produced using *C. splendens* leaf extract is shown in Fig. 10. The specific surface area of AgNPs calculated using the multipoint BET equation is 44.574 m^2g^{-1}. Assuming that the particles have spherical morphology, the average particle size can be estimated by the equation $D=6/(S_{BET}\times\rho_p)$, where, S_{BET}=BET surface area and ρ_p=particle density (3,059 kgm^{-3}) [50]. Thus, the average particle size of AgNPs is about 44 nm [D=6/(44.574×1000×3059)=44 nm]. This is in good accordance with the particle size range obtained from TEM and XRD analysis.

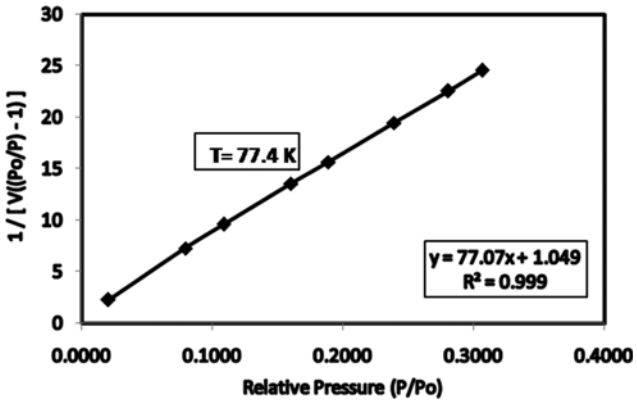

Fig. 10. BET plot of AgNPs.

12. Antibacterial Assay

The antibacterial potency of AgNPs against various airborne microbes using well diffusion method is shown in Fig. 11. *P. aeruginosa* and *B. subtilis* are used as a test strains for gram-negative and gram-positive bacteria, respectively. Fig. 11(a) shows that AgNPs have high antibacterial potency against gram-negative bacteria. This is due to the thin cell wall of gram-negative bacteria composed of single or double layer of peptidoglycans. In comparison to Fig. 11(a), a moderate antibacterial potency of AgNPs against the gram-positive bacteria is shown in Fig. 11(b). This is due the rigid cell wall of gram-positive bacteria composed of multiple lay-

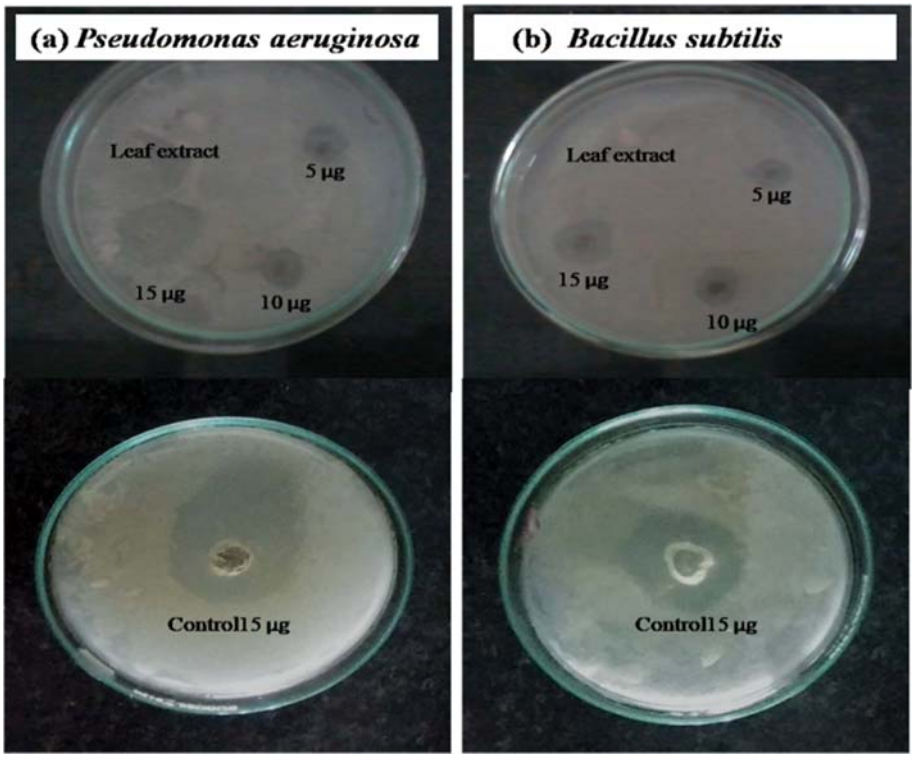

Fig. 11. Antibacterial activities of AgNPs against airborne microorganisms.

Table 4. Mean ZOI of AgNPs against airborne microorganisms

S. No.	Microorganisms	Concentration of AgNPs used (μg/mL)	Zone of inhibition (nm) (Mean of triplicates)
1	*P. aeruginosa*	5	12
		10	13
		15	19
		Leaf extract (15)	00
		Control (15)	22
2	*B. subtilis*	5	10
		10	12
		15	15
		Leaf extract (15)	00
		Control(15)	17

ers of peptidoglycan, which makes the penetration of AgNPs difficult [51].

The antibacterial potency of synthesized AgNPs against different microorganisms was tested and the results are in Table 4. The table shows the mean zone of inhibition (ZOI) around each well with AgNPs in different concentrations. The highest antibacterial potency against *P. aeruginosa* was observed at concentrations of 15 μg (19 mm) followed by 10 μg (13 mm) and 5 μg (12 mm). The highest antibacterial potency against *B. subtilis* was observed at concentrations of 15 μg (15 mm) followed by 10 μg (12 mm) and 5 μg (10 mm). The results from Table 4 suggest that the ZOI increases with increasing concentration of AgNPs. The well filled with *C. splendens* extract (15 μg/mL) did not show any ZOI, which implies that at a very low concentration, the extract alone is not antibacterial. The control well filled with 15 μg/mL of standard antibiotic Amoxicillin 500 mg exhibited a ZOI of 22 mm and 17 mm against *P. aeruginosa* and *B. subtilis*, respectively. The AgNPs due to their nano size easily penetrate into the microbial cell and hinder the intracellular processes such as synthesis of DNA, RNA, and protein. The killing of AgNPs with bacteria depends on its surface area of interaction on the cell wall. The AgNPs interaction on the cell surface area increases as the nanoparticle size decreases [52]. Therefore, smaller AgNPs have more bactericidal activity than the larger nanoparticles. Currently, the antimicrobial mechanism of activity of AgNPs is partially known. The positive charge AgNPs can bind to the negatively charged microorganisms by electrostatic attraction [53]. AgNPs strongly bind with the cell wall of microorganism, creating pits in the cell wall leading to the leakage of the cell and eventually the cell death [54].

13. Determination of Growth Curve

Antibacterial action of AgNPs and *C. splendens* was determined using the growth curve method. The *C. splendens* extract shows a steady increase in OD of both bacterial cultures, indicating rapid

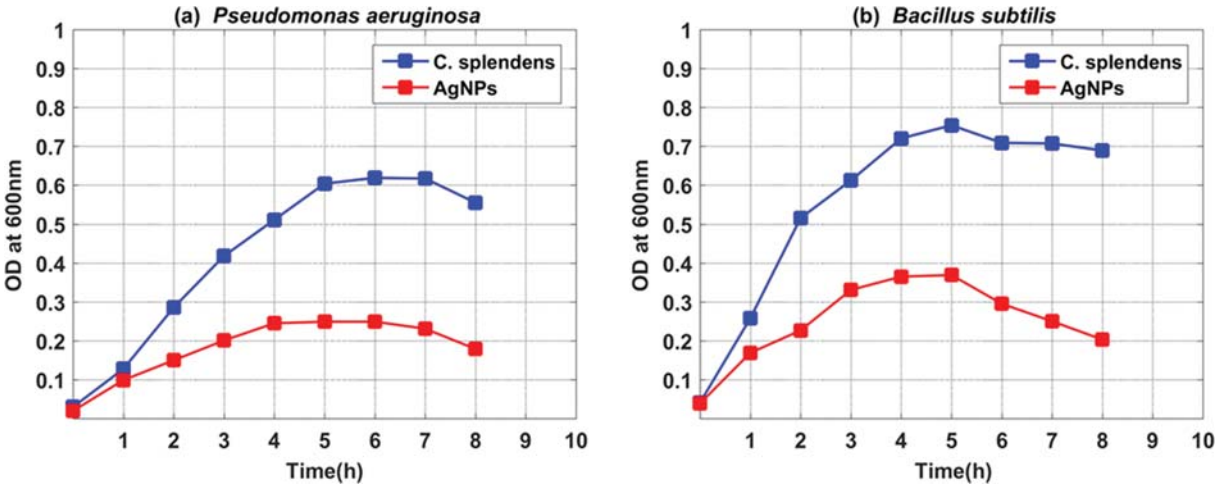

Fig. 12. Growth curve of AgNPs against airborne microorganisms.

Table 5. Antioxidant activity of plant extract and AgNPs by DPPH

S. No.	Compound	Absorbance	Absorbance at 517 nm		
			5 μg/mL	10 μg/mL	15 μg/mL
1	Control	$A_{control}$	0.9524±0.01	0.9524±0.01	0.9524±0.04
2	*C. splendens*	A_{sample}	0.631±0.01	0.313±0.03	0.294±0.05
		%AA	33.80	67.19	69.14
3	AgNPs	A_{sample}	0.459±0.07	0.154±0.02	0.145±0.03
		%AA	51.83	83.85	84.75
4	Ascorbic acid (standard)	A_{sample}	0.5130±0.04	0.1862±0.05	0.1593±0.04
		%AA	46.14	80.45	83.27

bacterial growth. The fabricated AgNPs demonstrates a relative decrease in OD reducing the growth of both *P. aeruginosa* and *B. subtilis* (Fig. 12). These results are in good agreement with the results from the antibacterial assay.

14. Antioxidant Assay

The DPPH assay is broadly employed to estimate the antioxidant potency of the compounds capable of scavenging the free radicals since it is a simple method [55]. The DPPH is considered as a stable free radical as it has an unpaired electron, which gives a violet color to the DPPH solution. When a compound having a donor of hydrogen atom is added to the DPPH solution, it scavenges the DPPH free radical, resulting in a color change of the solution from violet to yellow.

The antioxidant activity of each sample, reported in Table 5, shows that the synthesized AgNPs are better antioxidants. Further, Table 5 reveals that there was a dose-dependent increase in the percentage of antioxidant activity (%AA) of leaf extract and their synthesized AgNPs. The recorded value (%AA) for the *C. splendens* extract (5 μg/mL) was 33.80 and this value was increased to 69.14 when the concentration was increased to 15 μg/mL. However, the (%AA) values recorded for AgNPs were 51.83 for the concentration of 5 μg/mL and it increased to 84.75 for the concentration of 15 μg/mL. The DPPH assay of fabricated AgNPs, in comparison with the ascorbic acid, exhibits a promising antioxidant activity.

CONCLUSIONS

We have discussed the synthesis of AgNPs using leaf extract of *C. splendens*. The synthesized AgNPs have been well characterized using UV-vis spectroscope, zeta potential, TEM, XRD, XPS, BET and FTIR analysis. In UV-vis analysis, the completion of AgNPs synthesis time is faster (15 min) for PTH leaf extract compared to HW leaf extract. The reaction of AgNPs formation via *C. splendens* follows pseudo first-order kinetic model. Zeta potential value of −26.8 mV confirmed the high stability of PTH AgNPs in colloidal solution. The TEM analysis revealed that the PTH leaf extract produces spherical AgNPs with little aggregation and smaller particle size (~46 nm). The AgNPs synthesized with HW leaf extract showed more aggregations with average particle size ~58 nm. Compared to recent studies on the biosynthesis of AgNPs, the PTH method is observed to be a fast method producing AgNPs with better characteristics. Hence, we conclude that AgNPs synthesized with PTH *C. splendens* extract are superior compared to HW *C. splendens* extract. Due to their stable nature, our future studies will include the coating of the prepared AgNPs on air filter membranes and testing its efficiency against airborne pathogens.

ACKNOWLEDGEMENTS

The authors thank the Department of Chemical Engineering, A.C Tech, Anna University.

REFERENCES

1. S. K. Sahoo, R. Misra and S. Parveen, *In Nanomedicine in Cancer*, 73 (2017).
2. N. R. Shiju and V. V. Guliants, *Appl. Catal. A Gen.*, **356**, 1 (2009).
3. Y. Ju-Nam and J. R. Lead, *Sci. Total Environ.*, **400**, 396 (2008).
4. X. F. Zhang, Z. G. Liu, W. Shen and S. Gurunathan, *Int. J. Mol. Sci.*, **17**, 1534 (2016).
5. H. Duan, D. Wang and Y. Li, *Chem. Soc. Rev.*, **44**, 5778 (2015).
6. S. Prabhu and E. K. Poulose, *Int. Nano Lett.*, **2**, 32 (2012).
7. R. Shrestha, D. R. Joshi, J. Gopali and S. Piya, *Nepal J. Sci. Technol.*, **10**, 189 (2009).
8. A. Chahardoli, N. Karimi and A. Fattahi, *Adv. Powder Technol.*, **29**, 202 (2018).
9. M. Balamurugan and S. Saravanan, *J. Inst. Eng. India Ser. A*, **98**, 461 (2017).
10. M. Kumar and M. P. Sinha, *Not. Sci. Biol.*, **9**, 443 (2017).
11. D. Elumalai, M. Hemavathi, C. V. Deepaa and P. K. Kaleena, *Parasite Epidemiol. Control*, **2**, 15 (2017).
12. S. Asha, P. Thirunavukkarasu and S. Rajeshkumar, *Int. J. Pharmaceut. Res.*, **9**, 32 (2017).
13. K. Das, R. K. S. Tiwari and D. K. Shrivastava, *J. Med. Plants Res.*, **4**, 104 (2010).
14. S. N. Ingole, *Biodiversitas*, **12**, 146 (2011).
15. R. K. Jai, *Adv. Bio. Res.*, **1**, 84 (2010).
16. A. H. Shehata, M. F. Yousif and G. A. Soliman, *Egypt J. Biomed. Sci.*, **7**, 145 (2001).
17. N. R. Mshana, D. K. Abbiw, I. Addae-Mensah, E. Adjanohoun, M. R. A. Ahyi, J. A. Ekpere, E. G. Enow-Orock, Z. O. Gbile, G. K. Noamesi, M. A. Odei and H. Odunlami, Traditional medicine and pharmacopoeia. Contribution to the revision of ethnobotanical and floristic studies in Ghana. Organization of African Unity/Scientific, Technical & Research Commision, Accra. (2000).
18. H. M. Burkill, The useful plants of west tropical Africa Royal Botanic Gardens. *Kew*, UK, 130 (1985).
19. S. Y. Gbedema, K. Emelia, A. Francis, A. Kofi and W. Eric, *Pharmacognosy Res.*, **2**, 63 (2010).
20. S. Ahmed, L. Swami and S. Ikram, *J. Radiat. Res. Appl. Sci.*, **9**, 1 (2016).
21. W. Brand-Williams and M. E. Cuvelier, *LWT-Food Sci. Technol.*, **28**, 25 (1995).
22. T. Kumar and V. Jain, *Scientifica*, **2015**, 1 (2015).
23. M. Jeyaraj, M. Rajesh, R. Arun, D. Mubarak Ali, G. Sathishkumar, G. Sivanandhan, G. K. Dev and M. Manickavasagam, *Colloids Surf., B: Biointerfaces*, **102**, 708 (2013).
24. M. Noginov, G. Zhu, M. Bahoura, J. Adegoke, C. Small, B. A. Ritzo, V. P. Drachev and V. M. Shalaev, *Appl. Phys. B*, **86**, 455 (2007).
25. J. Clark and G. Gunawardena, *The Beer-Lambert Law*, Chemistry Libretexts (2016).
26. J. Clark, *Absorption spectra- The Beer-Lambert Law*, Chemguide (2016).
27. K. Ronson, *Nano Composix*, **1**, 1 (2012).
28. E. K. Elbeshehy, A. M. Elazzazy and G. Aggelis, *Front. Microbiol.*, **6**, 453 (2015).
29. A. Bécue and A. A. Cantú, *Fingermark detection using nanoparticles*, 307 (2012).
30. D. S. Balaji, S. Basavaraja, R. Deshpande, D. B. Mahesh, B. K. Prabhakar and A. Venkataraman, *Colloids Surf., B: Biointerfaces*, **68**,

88 (2009).
31. I. B. Sorokulova, I. V. Pinchuk, M. Denayrolles, I. G. Osipova, J. M. Huang, S. M. Cutting and M. C. Urdaci, *Digest. Dis. Sci.*, **53**, 954 (2008).
32. R. Ogórek, A. Lejman, W. Pusz, A. Miłuch and P. Miodyńska, *Mikol. Pol.*, **19**, 80 (2012).
33. J. U. Shareef, M. N. Rani, S. Anand and D. Rangappa, *Mater. Today: Proc.*, **4**, 11923 (2017)
34. K. Vahabi, G. A. Mansoori and S. Karimi, *Insciences J.*, **1**, 65 (2011).
35. S. Hashemi, M. H. Givianrad, A. M. Moradi and K. Larijani, *Indian J. Geo-Mar. Sci.*, **44**, 1415 (2015).
36. J. J. Coppen, *Eucalyptus: the genus Eucalyptus* (2002).
37. I. Johnson and H. J. Prabu, *Int. Nano Lett.*, **5**, 43 (2015).
38. N. Agasti, *Am. J. Nanomater.*, **2**, 4 (2014).
39. B. D. Cullity, Elements of X-ray diffraction (1978).
40. A. M. Fayaz, K. Balaji, M. Girilal, R. Yadav, P. T. Kalaichelvan and R. Venketesan, *Nanomedicine: NBM*, **6**, 103 (2010).
41. D. Michael, How to Read IR Spectrums, Sciencing (2017).
42. A. J. Kora and R. B. Sashidhar, *Carbohydr Polym.*, **82**, 670 (2010).
43. S. Kaviya and J. Santhanalakshmi, *Mater. Lett.*, **67**, 64 (2012).
44. H. Schulz, *Vib. Spectrosc.*, **43**, 13 (2007).
45. J. Huang, Q. Li, D. Sun, Y. Lu, X. Yang, H. Wang, Y. Wang, W. Shao, N. He and J. Hong, *Nanotechnology*, **18**, 105104 (2007).
46. H. Bakhshi, H. Yeganeh, S. Mehdipour, A. Shokrgozar, A. Yari and N. Saeedi, *Mater. Sci. Eng.: C*, **33**, 153 (2013).
47. R. Sukirtha, M. Priyanka, J. Antony, R. Thangam, P. Gunasekaran and M. Krishnan, *Process Biochem.*, **47**, 273 (2012).
48. S. Li, Y. Shen, A. Xie, X. Yu and L. Qiu, *Green Chem.*, **9**, 852 (2007).
49. L. Zhang, Z. Wu, L. Chen, L. Zhang, X. Li, H. Xu, H. Wang and G. Zhu, *Solid State Sci.*, **52**, 42 (2016).
50. J. S. Prasad, V. Dhand, V. Himabindu and Y. Anjaneyulu, *Int. J. Energy Environ.*, **1**, 607 (2010).
51. S. Shrivastava, T. Bera, A. Roy, P. Ramachandrarao and D. Dash, *Nanotechnology*, **18**, 225103 (2007).
52. H. J. Yen and S. H. Hsu, *Small*, **5**, 1553 (2009).
53. T. C. Dakal, A. Kumar and R. S. Majumdar, *Front. Microbiol.*, **7**, 1831 (2016).
54. L. Wang and C. Hu, *Int. J. Nanomedicine*, **12**, 1227 (2017).
55. H. Fenglin, *Fitoterapia*, **75**, 14 (2004).